DOI: 10.1007/s11099-016-0646-3 PHOTOSYNTHETICA 54 (4): 589-597, 2016

Girdling interruption between source and sink in *Quercus pubescens* does not trigger leaf senescence

V. HOLLAND[*,**,+], L. FRAGNER[***], T. JUNGCURT[**], W. WECKWERTH[***], and W. BRÜGGEMANN[*,**]

Biodiversity and Climate Research Centre (BiK-F) Frankfurt, Senckenberganlage 25, 60325 Frankfurt, Germany[*]
Department of Ecology, Evolution and Diversity, Goethe University, Max-von-Laue-Str. 13, 60438 Frankfurt, Germany[**]
Department of Ecogenomics and Systems Biology, University of Vienna, Althanstr. 14, 1090 Wien, Austria[***]

Abstract

Metabolite changes and senescence behaviour after mechanical phloem girdling were studied in leaf tissue of *Quercus pubescens*. Sugar accumulation is not only considered to be an important part of several developmental signalling pathways, but is also seen as one of the basic triggers for senescence induction, or at least an obligatory accessory phenomenon. Our survey showed that an accumulation of the soluble sugars, glucose and fructose, was not on its own obligatorily connected with the induction of leaf senescence, since no indication or even an onset of senescence could be observed during the course of the experiment. Instead, we observed an inhibition of leaf development with a decrease of photosynthesis and a slow-down of development in nearly all chlorophyll *a* fluorescence analysis parameters using the JIP-test. We detected a change of metabolites linked to oxidative stress, possibly due to an overexcitation of the developmentally inhibited photosynthetic apparatus.

Additional key words: chlorophyll fluorescence; climate change; metabolomics; JIP-test; PEA; SPAD.

Introduction

Many developmental processes in plants are regulated by metabolites. Soluble carbohydrates play a major role in seed germination and in the induction of flowering and senescence (Gibson 2005) and in stress response (Wingler and Roitsch 2008). Sugar accumulation inhibits the expression of some photosynthesis genes (Jang and Sheen 1994). Photosynthesis is generally considered to be regulated by a negative feedback inhibition loop in the source-sink interaction (Noodén and Guiamét 1989). In single-rooted *Amaranthus* leaves, a model for a severely sink-limited plant system, Sawada *et al*. (2002) found an increase in soluble sugars and starch, concomitant with a coordinated decline in activities of photosynthetic dark reactions enzymes. Taken together, these results suggest that (*1*) manipulation (or natural modification) of source/sink relationships between leaves and sink organs may strongly influence carbohydrate accumulation in source leaves, and (*2*) that the signalling participation of carbohydrate concentrations in developmental processes may induce senescence processes. Under natural conditions, carbohydrate accumulation is induced by abiotic stress or age-dependent processes. We could show that the induction of senescence in downy oak (*Quercus pubescens* Willd.) under natural autumn conditions goes along with carbohydrate accumulation, when the plants were exposed to drought or frost events. In well-watered and frost-free plants, senescence occurred independently of carbohydrate accumulation (Holland *et al*. 2015). We concluded from our findings in intact plants that carbohydrate accumulation during autumn is not a necessary prerequisite for leaf senescence. In order to elucidate whether artificial increase of leaf carbohydrates in *Q. pubescens* can be considered as a sufficient trigger for the induction of senescence, we studied a system of artificial sink limitation by phloem interruption of intact twigs using the girdling technique. We hypothesized that sink deprivation of anatomically fully expanded source leaves in downy oak would lead to carbohydrate accumulation and possibly induce leaf senescence, visible in a decrease of chlorophyll content and changes in the photosynthetic apparatus.

Received 29 September 2015, *accepted* 19 May 2016, *published as online-first* 5 August 2016.
[+]Corresponding author; phone: +49.69.798.42118, e-mail: vholland@gmx.de
Abbreviations: C – control; Chl – chlorophyll; DM – dry mass; DOE – day of experiment; F_0 – minimal fluorescence yield; F_m – maximal fluorescence yield; F_v/F_m – maximum quantum yield of PSII photochemistry; FM – fresh mass; G – girdle; md – measuring date; MCW – methanol:chloroform:water mixture; MSTFA – N-methyl-N-trimethylsilyltrifluoroacetamid; P_N – net photosynthetic rate; RWC – relative water content; TM – turgid mass.
Acknowledgement: The present study was financially supported by the research funding programme "LOEWE – Landes-Offensive zur Entwicklung Wissenschaftlich-ökonomischer Exzellenz" of Hesse's Ministry of Higher Education, Research, and the Arts.

Materials and methods

Plant material, sugar accumulation and sampling dates: Ten specimens of *Q. pubescens* (seven years old and approx. 2.5 m high) were grown in a common garden experiment with other oak taxa. The experimental site at the Goethe University Frankfurt, Germany was located at 50°10'09,79''N 8°37'50,37''E. Climate conditions were monitored continuously using an *iMetos sm SMT280* climate station (*Pessl Instruments*, *Weiz*, Austria). The first day of experiment (DOE) was 3 June, 2013 (DOE 0) and the girdle experiment ended 21 d later on 24 June, 2013 (DOE 20). For all measurements, south-exposed sun leaves were collected. Mechanical girdling or steam girdling allows the manipulation of leaf carbohydrate contents by interruption of sieve tubes (Parrott *et al*. 2005), without influencing the water supply of the organ. In order to determine the best time point for the girdling intervention and to figure out the best girdling method preventing the plants from damage, preliminary experiments were performed (data not shown). Girdling was carried out along the twigs, 10 cm from the initiation of the apical leaf. The girdled tissue, a 1-cm wide ring of bark, was removed around the twig using razor blades and magnifier. To prevent fungal infections, wound wrapping was omitted.

Determination of the relative water content (RWC): A crucial moment in the process of girdling is the removal of the sieve tube tissue. It is important to remove the phloem carefully without damaging the xylem. To exclude false results by xylem injury and restricted water supply, RWC was monitored on sampled leaves during the whole experiment, as the resulting drought stress would lead to a subsequent modification of the leaf metabolome. The relative water content was determined for every leaf sample taken (n = 10) according to Barrs and Weatherley (1962). Leaf discs of 1.27 cm² fresh leaf tissue were weighed (fresh mass, FM), then weighed again after saturation by soaking in water in microcentrifuge tubes at 4°C overnight and removing any adhered water droplets with tissue paper (turgid mass, TM). Finally, the samples were weighted again after drying in an oven at 80°C overnight (dry mass, DM). The RWC was calculated according to the following equation:

$$\mathrm{RWC}\ [\%] = \frac{(\mathrm{FM} - \mathrm{DM})}{(\mathrm{TM} - \mathrm{DM})} \times 100$$

Chlorophyll (Chl) content was assessed by *SPAD 502 plus* readings (*Konica-Minolta*, Munich, Germany). The *SPAD 502 plus* is a portable Chl meter that assesses leaf absorbance at 650 nm (red) and at 940 nm (near-infrared). It displays so-called SPAD readings, which are calculated using the 940 nm absorbance as a reference for structural (*i.e*. nonpigment associated) absorption. The device thus measures the relative Chl content of the sample non-destructively. The *in vivo* SPAD readings were calibrated against leaf Chl contents observed from *in vitro* acetone extracts of the identical leaves. The extractions were also performed to assess the Chl *a*/*b* ratios. Extracts were prepared under low light [<1 µmol(quanta) m^{-2} s^{-1}] with liquid nitrogen and measured according to Lichtenthaler (1987) with a UV-visible spectrophotometer (*U-2900*, *Hitachi High-Technologies Corporation*, Tokyo, Japan).

Chl fluorescence: PSII functionality was assessed by the JIP-test with a portable fluorimeter (*Pocket-PEA*, *Hansatech Instruments Ltd*., King's Lynn, UK) according to Strasser *et al*. (2000, 2004). Measurements were carried out on dark-adapted leaves, with all primary acceptor Q_A molecules fully oxidized. A red saturating light flash induced fluorescence to ensure the reduction of all acceptors. The JIP-test parameters derived from the original induction curves were calculated using the *PEA Plus 1.0.0.1* software (*Hansatech Instruments Ltd*., King´s Lynn, UK) or using *Excel 2010* (*Microsoft*, Albuquerque, USA). Formulae according to Strasser *et al*. (2000) using the 50 µs fluorescence level as F_0 are explained in Table 1. The individual induction curves (n = 15) were averaged for each taxon and sampling date. The averaged fluorescence induction curves from the measurements in the beginning of September were used as references for comparison with the averaged curves from the following dates to calculate double normalized (between F_0 and F_m) differential induction curves:

$$[\Delta V_{OP} = [(F_t - F_0)_{md}/(F_m - F_0)_{md}] - [(F_t - F_0)_{DOE\ 0}/(F_m - F_0)_{DOE\ 0}],$$

with md – measuring date and DOE 0 – control date] (*e.g*. Jiang *et al*. 2006, Yordanov *et al*. 2008).

Photosynthetic activity: Gas-exchange rates were measured on randomly selected, south-exposed leaves with a Clark oxygen electrode in an *LD 2/3* setup (*Hansatech*, King's Lynn, UK). For calculation of the maximum photosynthetic capacity (P_{max}) at a saturating CO_2 concentration, leaf discs were excised with a cork borer. O_2 production was measured for 10 min, at 25°C, 900 µmol(quantum) $m^{-2}s^{-1}$ PAR (emitted by the *LH36/2R* light source) under 2% O_2, 4.5% CO_2 in N_2, following 10 min of dark adaptation.

Table 1. Explanation of Chl fluorescence parameters and derived physical variables.

Used fluorescence parameters	
$F_0 = F_{50\mu s}$	Fluorescence intensity at 50 µs
F_m	Maximal fluorescence intensity
F_t	Fluorescence at time t
$F_{150\mu s}$	Fluorescence intensity at 150 µs
$F_{300\mu s}$	Fluorescence intensity at 300 µs
F_J	Fluorescence intensity at 2 ms
M_0	Initial slope of the induction curve. $M_0 = 4\ (F_{300\mu s}F_0)/(F_m - F_0)$
PI_{abs}	Performance index on absorption basis. Efficiency of energy conservation from absorbed photons to reduction of intersystem electron carriers. $PI_{abs} = (RC/ABS)\ [\phi P_0/(1 - \phi P_0)]\ [(1 - V_J)/(1 - (1 - V_J))]$
V_J	Relative variable fluorescence at 2 ms. $V_J = (F_{2ms} - F_0)/(F_m - F_0)$
$1–V_I$	Relative amplitude of IP-phase in comparison to control. $1 - V_I = \Delta V_{IP} = (F_m - F_I)/(F_m - F_0)$
$V_{OJ,\ 300\mu s}$	Relative variable fluorescence of the OJ-phase at 300 µs. $V_{OJ,300\mu s} = (F_{300\mu s} - F_0)/(F_{2ms} - F_0)$
Specific fluxes per active PSII reaction centre	
DI_0/RC	Dissipation flux, $DI_0/RC = ABS/RC – TR_0/RC$
ET_0/RC	Electron transport flux further than Q_A. $ET_0/RC = M_0\ (1/V_J)\ (1 - V_J)$
RC/ABS	Reaction centres per absorption $RC/ABS = \phi P_0\ (V_J/M_0)$
RE_0/RC	Electron flux leading to the reduction of the PSI end acceptor. $RE_0/RC = M_0\ (1/V_J)\ (1 - V_I)$
TR_0/RC	Trapped energy flux leading to a reduction of Q_A. $TR_0/RC = M_0\ (1/V_J)$
Quantum efficiency/ Flux ratios	
ϕD_0	The probability that the energy of an absorbed photon is dissipated as heat. $\phi D_0 = 1 - \phi P_0$
ϕE_0	Quantum yield of electron transport expresses the probability that an absorbed photon leads to an electron transport further than Q_A. $\phi E_0 = ET_0/ABS$
ϕP_0	Quantum yield of primary photochemistry expresses the probability that an absorbed photon leads to a reduction of Q_A. $\phi P_0 = TR_0/ABS = (F_m - F_0)/F_m$
ϕR_0	The probability that an absorbed photon leads to a reduction of the PSI end acceptor. $\phi R_0 = RE_0/ABS$
Ψ_0	The probability that an absorbed photon leads to a reduction further than Q_A.

Metabolomics: Metabolome analysis of the leaf tissue was used to study the accumulation of soluble carbohydrates in the source tissue as a response of the plants to girdling (Schauer and Fernie 2006 and citations therein). For GC–MS analysis a protocol slightly modified according to Weckwerth *et al*. (2004) was used. Two south-exposed sun leaves of control and stress treatment of each plant from four points in time (3 June 2013 = DOE 0; 7 June 2013 = DOE 3; 12 June 2013 = DOE 8; 20 June 2013 = DOE 16) were harvested and immediately frozen in liquid nitrogen, ground to a fine powder at 30 Hz for 1 min using 25-ml stainless steel grinding jars in a Retsch grinder (*MM 400*, *Retsch GmbH & Co.*, Haan, Germany), and lyophilized. For the extraction, 5–6 mg of DM was weighed in 2-ml Eppendorf reaction tube. The leaf tissue was extracted at 4°C with 800 µl of ice cold extraction mixture (methanol:chloroform:water = MCW 2.5:0,5:1 v/v/v), agitated for 10 s, incubated for 15 min on ice and thoroughly vortexed. The samples were centrifuged (4 min, 4°C, 14,000 × *g*) and the supernatant (containing the metabolites) was transferred to a new 2-ml reaction tube. The extraction was repeated with 400 µl of MCW and the supernatants were combined. For the phase separation, 400 µl of water (Milli Q quality) was added, the samples were agitated and centrifuged again (2 min, 4°C, 14,000 × *g*). The upper polar phase was transferred to a new Eppendorf tube. The samples were evaporated to dryness in a speed-vac concentrator (*Scan Vac*, *LaboGene APS*, Denmark). The dry pellet was derivatized by adding 20 µl of a 40 mg methoxyamine hydrochloride per 1 ml of pyridine solution and incubated on a thermo shaker (30°C, 90 min). Then 80 µl of a silylation mixture was added followed by incubation for 30 min at 37°C. This mixture contained N-methyl-N-trimethylsilyltrifluoroacetamid (MSTFA) (*Machery Nagel*, Düren, Germany) spiked with retention index markers for calculation. Therefore, 30 µl of a standard solution containing even numbered alkanes from C10 to C40 dissolved in hexane at the concentration of 50 mg l^{-1} (*Sigma Aldrich Handels Gmbh*, Austria) were added to 1 ml of MSTFA. The derivatized sample (70 µl) was transferred to GC-microvials with microinserts and closed with crimp caps (Strehmel *et al*. 2008). All samples were extracted, derivatized and measured in random order. Each batch contained not more than 24 samples and at least 1 blank was included, respectively.

GC–TOF/MS analysis: GC–MS measurements were carried out on an *Agilent 6890* gas chromatograph coupled to a *LECO Pegasus 4D* mass spectrometer (*LECO Corporation,* USA). Injection was performed splitless with a 4 mm inner diameter tapered liner containing deactivated glass wool at an injection temperature of 230°C. Components were separated on an *Agilent HP-5MS* column (30 m length, 0.25 mm diameter, 0.25 µm film). The initial oven

temperature was 70°C (hold) for 1 min, followed by a ramp of 9°C per min to 330°C final temperature, which was held for 8 min. Electron impact ionisation was performed at 70 eV, data acquisition rate was set to 20 spectra s^{-1} at a mass range of 40–600 Th and the detector voltage was 1,550 V. The on-board *LECO Chroma-TOF* software capable of mass spectral deconvolution, baseline correction, and automated peak detection processed the obtained raw data. Compounds were annotated by matching of deconvoluted spectra to mass spectral databases, an in house library and the *Golm Metabolome Database* (Kopka *et al*. 2005), with a minimum match factor of 850. Further support of annotation was obtained by manual comparison of retention indices (Strehmel *et al*. 2008). A reference list of peaks was created using representative chromatograms and all samples were processed with this reference and peak areas of specific quant masses were extracted of all samples and exported into an *Excel* worksheet (Doerfler *et al*. 2013).

Statistics: For comparison of all data from different time points an unpaired *t*-test with *Welch*'s correction was used. For comparison of data sets from the same time point but different treatments a paired *t*-test was used. Statistical analyses were carried out using *GraphPad PRISM 5.04* (*GraphPad Software, Inc*., La Jolla, CA, USA).

Results

To investigate leaf development of the different twigs, we monitored different physiological parameters of the leaves during the first 20 d after the girdling intervention. The relative water content was taken as internal control of the girdling intervention itself, to ensure the intactness of the water supply of the twigs. The relative Chl content was monitored to investigate, whether the leaves showed signs of senescence during the experiment. Both relative Chl content of the leaves depicted as SPAD value (Fig. 1*A*) as well as the relative water content (Fig. 1*B*), did not differ significantly between the control (C) and the girdled (G) group at any time during the experiment. The photosynthesis linked parameters PI_{abs} (Fig. 1*C*) and the photosynthetic rate (Fig. 1*D*) of the C and the G group showed first significant changes on DOE 3. The G group showed lower values of these parameters. The averaged Chl fluorescence induction curves (Fig. 2) of all leaves from the groups C and G showed nearly identical curve patterns on the control date (DOE 0). On DOE 16, the C twigs showed significantly higher F_m values than on DOE 0. In the curves on DOE 16, the J-step nearly disappeared in the C and G twigs. In order to study differential developmental patterns between the C and G twigs in the time course, we calculated double normalized curves [$V_t = (F_t - F_0)/(F_m - F_0)$] and compared them between the groups by subtraction, leading to so-called ΔV_{OP} curves (Fig. 3). The ΔV_{OP} curve changed considerably during the experiment and revealed a multipeak behaviour. Initially, a peak at 1–2 ms was present, followed by a peak at 10–20 ms with a shoulder around 100 ms. In order to have a closer look at the physiological processes responsible for the differential development of the curve shapes, we summarized single JIP-test parameters in a spider plot (Fig. 4). These parameters represent different processes/components of the electron transport chain. For this purpose we selected two dates: DOE 0 as a control, and DOE 16, when the girdling had visible effects on the JIP-test parameters. Between the groups C and G on DOE 0 no significant differences could be observed. During the experiment, all

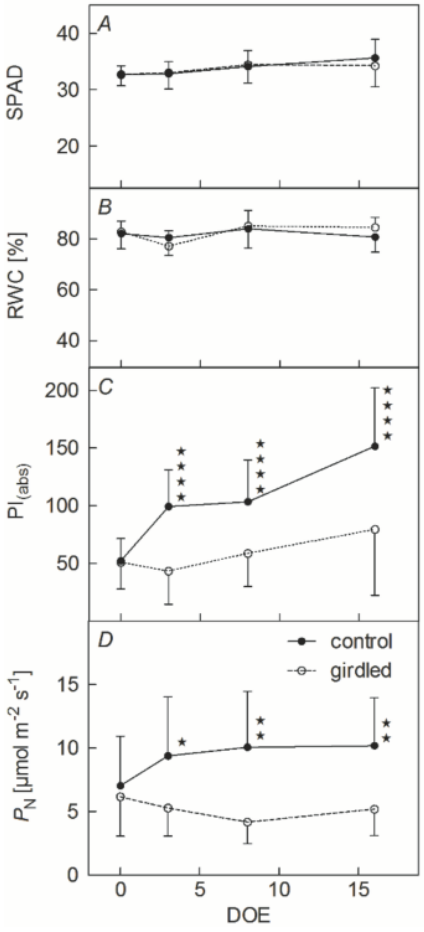

Fig 1. (*A*) Relative chlorophyll (Chl) content (SPAD), (*B*) relative water content in % (RWC), (*C*) performance index (PI_{abs}), and (*D*) net photosynthetic rate (P_N) of *Quercus pubescens* in the course of the experiment in summer 2013. *Continuous black line* − control group, *dashed line* − girdled group; day of experiment (DOE) 0–20 (n = 10; means ± SD). Where indicated, parameters of G twigs differ significantly from those of C twigs at * − p<5%, ** − p<1%, *** − p<0.1%, **** − p<0.01%.

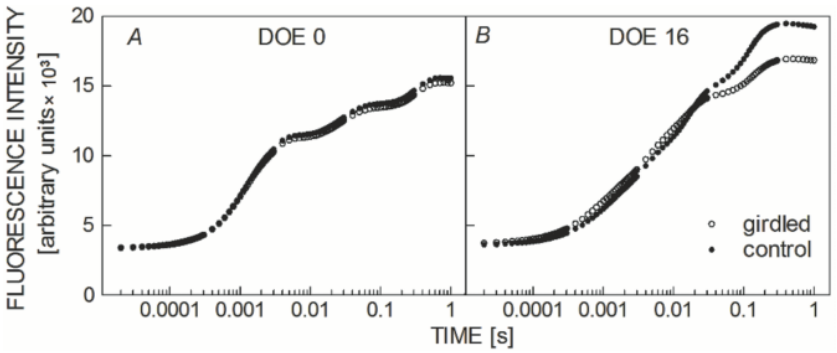

Fig. 2. Averaged relative chlorophyll fluorescence induction curves (n = 30), on (A) day of experiment (DOE) 0 and (B) DOE 16 from C and G twigs.

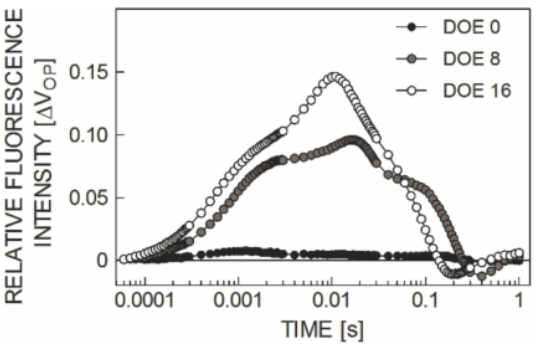

Fig. 3. Averaged (n = 30) differential chlorophyll fluorescence induction curves of leaves from G twig compared to C twig on three dates during experiment [days of experiment (DOE) 0, 8, 16]. Curves were double normalized to O (F_0).

leaves showed an increase in most of the depicted parameters as a consequence of further (physiological, not anatomical) leaf development. The C twigs revealed a significant increase of the performance index (PI_{abs}) by 200 % and of ΦR0, the quantum efficiency of the PSI end acceptor side reduction, by 40% from DOE 0 to DOE 16. These increases were accompanied by a significant decrease of ΦD_0, the maximum quantum efficiency of energy dissipation and RC/ABS, the density of active reaction centres per absorption unit. The girdled twigs showed similar changes of several parameters, but to a smaller extent or only by trend (ΦD_0).

In the metabolome analyses, a total of 90 peaks was analysed per sample. Since peaks were only further analysed when present in more than 50% of the samples, 46 substances remained to be further studied. Out of these, in Table 2, the 11 most important substances which were identified *via* GC–MS analysis, were listed. The concentrations of eight substances differed significantly between the groups on all time points during the experiment. Sucrose, prolin, and threonic acid showed no significant changes in their concentration. The most significant changes in metabolite concentrations were visible on

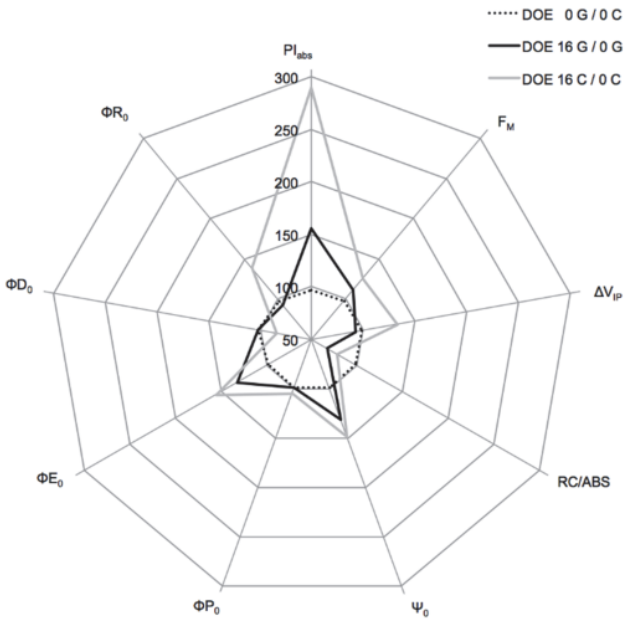

Fig. 4. Spider plot of JIP-test parameters (n = 30). *Dotted line* (•••) − C *vs*. G leaves on day of experiment (DOE) 0; *black line* – C at DOE 16 *vs*. C at DOE 0; *grey line* − G at DOE 16 *vs*. G at DOE 0.

DOE 16. In ascorbic acid and phenylalanine, transient changes occurred already on DOE 8, but were not detected again on a later date.

The contents of the soluble sugars (fructose, glucose, sucrose) detected by metabolome analysis in the time course of the experiment, are depicted in arbitrary units (Fig. 5). Strong significant changes in fructose and glucose contents between the samples of the G twigs in comparison to samples of the C twigs occurred on DOE 16, while on the other days of the experiment the contents stayed stable. Sucrose scattered stronger than fructose and glucose, but no significant changes could be detected between the C and G group.

Discussion

Xylem injury could lead to drought stress, which on its part may induce sugar accumulation in the leaves (Patakas and Noitsakis 2001, Holland *et al*. 2015) and thus falsify the results. None of the leaves of the differentially treated twigs showed any fluctuation of the RWC or a concentration decline of several known drought-stress relevant metabolites, such as threonine, valine, proline or malate (Sardans 2011), so drought stress could be excluded as a possible stressor (Fig. 1*B*). Measurements of the relative Chl content and the Chl fluorescence induction curves were conducted in order to investigate, whether the expected sugar accumulation of the girdling intervention in the leaves induced senescence. Other studies show that naturally occurring sieve tube occlusion and carbohydrate accumulation is often associated with Chl degradation (Jongebloed *et al*. 2004). In spinach, girdling-induced accumulation of sugars was associated with a decrease in Rubisco transcript levels and Chl and protein degradation (Krapp and Stitt 1995). However, the relative Chl content depicted as SPAD values (Fig. 1*A*), stayed stable in downy oak and showed no significant differences in the leaves of the C and G twigs in the present study. In order to screen the vitality of the plants and their developmental stage, measurements of photosynthetic O_2 assimilation (Fig. 1*D*) and Chl *a* fluorescence (Fig. 1*C*) were carried out. The O_2 assimilation rate of leaves from the G twigs in comparison to the leaves of the C twigs was only half as high on DOE 3 (Fig. 1*D*). Girdling or other sink subtractions increase starch contents and reduce photosynthesis (Iglesias *et al*. 2002). A decrease of photosynthetic metabolism was considered as one of the basic triggers for leaf senescence in monocarpic plants (Hensel *et al*. 1993). In barley, the inhibition of source-sink export through steam girdling and a following sugar accumulation in leaves resulted in an increased expression of senescence-associated genes like *SAG12* (Parrott *et al*. 2007). In a sugar accumulating *Arabidopsis* mutant, pho3, a large number of genes was increasingly expressed during developmental senescence (Lloyd and Zakhleniuk 2004). However, the differences were not only caused by a decreased photosynthesis of the leaves of the G twigs, but also by an increase in photosynthetic activity of the leaves of the C twigs. Increased values of photosynthesis may either indicate that the development of the leaves is not completed or that the control twigs try to compensate the breakdown of assimilate supply of the tree by the G twigs (Yordanov 1984, Yordanov *et al*. 2008). A closer look inside the photosynthetic apparatus using the JIP-test analysis supports the hypothesis of incomplete leaf development. This analysis allows separation of stress effects of individual steps of the electron transport chain (Strasser *et al*. 2000, 2004). A comparison of the fluorescence transients of the leaves from the C twigs between the beginning of the experiment DOE 0 and DOE 16 (Fig. 2) showed the typical changes of transients during the vegetation period due to leaf development; maximum fluorescence intensity F_m was increasing (Strivastava and Strasser 1999) while fluorescence intensity after 2 ms F_J (J-step) was proportionally decreasing during development (Jiang *et al*. 2006) in all leaves of both groups (Fig. 2*B*). Consequently, decreasing RC/ABS values can be seen in the spider plot (Fig. 4), *i.e*. the absorption flux per reaction centre increased (Strasser *et al*. 2004). The observation that the SPAD values remained stable during the measuring period imply that during leaf development rearrangements of pigment-bearing systems must have occurred, leading to a more efficient energy transfer to the RCs. A decreasing J-step points to a faster reoxidation

Table 2. Important (sucrose/prolin/threonic acid) or significantly changed leaf metabolites identified by GC–MS analysis of leaves from C and G twigs. *p* values calculated between G and C group on day of experiment (DOE) 0, 8, and 16. *Arrows* show the direction of regulation of the substances in the girdled twigs in comparison with the control twigs. *n* – the number of samples (out of nine per DOE), in which the named substance was unambiguously identified. NA – unknown substances, which were not annotated. The tag 'sum' in brackets behind the substances indicates multiple detections (peaks) obtained from the same substance by different derivation products during sample preparation.

Metabolite	DOE 0		DOE 8			DOE 16		
	n	*p* value	Change	*n*	*p* value	Change	*n*	*p* value
Ascorbic acid (sum)	9	NS	↓	9	0.0024		9	NS
Citric acid (sum)	9	NS	↓	9	0.0079	↓	9	0.0007
Fructose	9	NS		9	NS	↑	9	0.0009
Glucose (sum)	9	NS		9	NS	↑	9	0.0029
NA 8	9	NS		9	NS	↑	9	0.0007
Phenylalanine (sum)	7	NS	↓	6	0.0271		3	NS
Prolin (sum)	8	NS		6	NS		5	NS
Quinic acid	9	NS	↓	9	0.0008	↓	9	0.0026
Sucrose	9	NS		9	NS		9	NS
Threonic acid	9	NS		9	NS		9	NS
Viburnitol	9	NS		9	NS	↑	9	0.0022

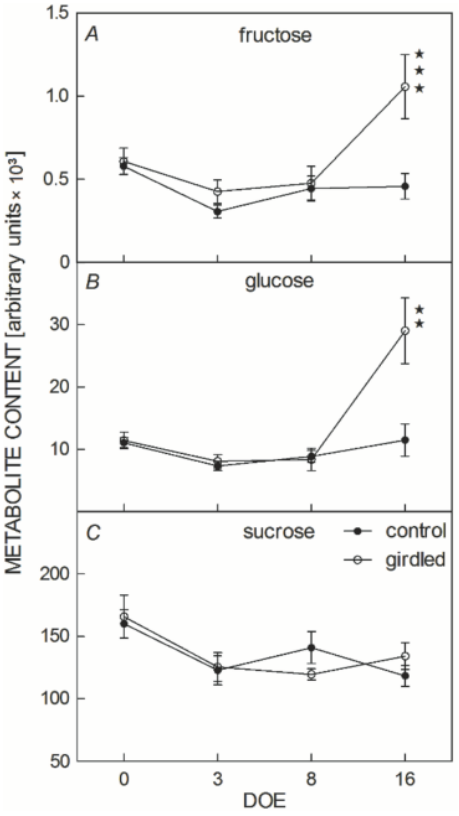

Fig. 5. Averaged metabolome contents [peak area mg^{-1}(DM)] of the soluble sugars – (*A*) fructose, (*B*) glucose, and (*C*) sucrose of leaves from G and C twigs on four dates during experiment [day of experiment (DOE) 0, 3, 8, 16; n = 9; means ± SE]. Where indicated, metabolites of G twigs differ significantly from those of C twigs at * − p<5%, ** − p<1%, *** − p<0.1%, **** − p<0.01%.

of Q_A and/or a bigger size of the PQ-pool (Joly *et al*. 2005) and thus a better electron transfer through the electron transport chain. The averaged relative Chl fluorescence induction curves (Fig. 2) reflected a deceleration of the development in the G twigs. Differences between the ΔV_{OP} curves of leaves from the C and G twigs were also attributable to the fact that F_m in the leaves of the C twigs changed to a larger extent than that in the leaves of the G twigs during the experiment, whereas F_0 stayed the same. The parameters depicted in the spider plot support these findings. An increase of the vitality parameter PI_{abs}, a term combining three components associated with light capturing and PSII electron transport [*i.e.* the density of reaction centres (RC/ABS), the quantum yield of light trapping (ΦP_0), and the probability that an absorbed photon leads to a reduction further than Q_A^- $(1 - V_J)$], was visible in all twigs. It was twice as high in the leaves of the C twigs as in the leaves of the G twigs. Most summarized parameters showed proceeding development of all leaves, but to a much lesser extent in the leaves of the G twigs. Interestingly, the developmental process as reflected in order of the creation of the photosynthetic apparatus was inverse to the degradation of the photosynthetic apparatus during senescence (Holland *et al*. 2014). Due to their direct relation ($\Phi D_0 = 1 - \Phi P_0$), the observed significant increase of the quantum yield of PSII electron transport to Q_A (ΦP_0) is linked to a significant decrease of the quantum efficiency of heat dissipation (ΦD_0) in the control leaves. In the G leaves, the quantum efficiency of heat dissipation as well as the light trapping did not change significantly during the experiment. The quantum efficiency of the reduction of the PSI end acceptor side (ΦR_0) as well as ΔV_{IP}, *i.e*. the relative amplitude of the I–P phase, which is linked to the content of PSI reaction centres (Ceppi *et al*. 2012), increased only in the C twigs. As judged from the change in the shape of the Chl fluorescence induction curve and the increasing performance index, the photosynthetic apparatus of both groups showed further development. However, in contrast to the C twigs, in which both the capacity of the photosynthetic apparatus for CO_2 fixation and the performance index strongly increased with time, the G twigs showed stagnation or decrease of the photosynthetic capacity (Fig. 1*C*,*D*). The girdling process disturbed the balance of source-sink relation between the leaves on the girdled twig and the rest of the plant. An increased source activity in relation to the effective sink activity usually results in starch and/or sugar accumulation in the leaves (*e.g*. Sawada *et al*. 1999). Metabolome analysis revealed no changes in sucrose contents, indicating that the physiological changes were not drought-related (Pinheiro *et al*. 2004, Rizhsky *et al*. 2004), but significantly elevated concentrations of the soluble sugars fructose and glucose in the G samples occurred on DOE 16.

Some photosynthesis genes are known to be sugar-repressible (Krapp *et al*. 1993, Webber *et al*. 1994). Krapp and Stitt (1995) found changes in the expression of photosynthesis genes in spinach due to sink demand through cold-girdling. Glucose is known to repress growth and leaf development in *Arabidopsis* (Xiao *et al*. 2000). Such effects may alter the "normal" development of the *Q. pubescens* leaves leading to higher photosynthetic activities, visible in the C group. It is also known that maximum photosynthetic activity in *Q. robur* can be acquired very late, *i.e.* between end of June and end of July (Morecroft *et al*. 2003), despite the apparently full morphological development of the leaves four weeks earlier. A slow-down of the developmental processes of the girdled twigs could lead to an overexcitation of the photosynthetic apparatus and oxidative stress. Radiation in mid summer is high and can lead to high rates of reactive oxygen species (ROS) in the cells, if the photosynthetic apparatus is not fully mature. ROS concentrations increase if their creation rate exceeds the capacity of antioxidants to reduce them (Baxter *et al*. 2007). The decreased contents of ascorbate and citrate on DOE 8 corroborate this fact. Ascorbate plays a major role in reducing oxidative stress, *e.g*. *via* the ascorbate-glutathione cycle. The stable content of threonate, a breakdown product of ascorbate,

pointed to an effective operation of ROS recycling. If the oxidative stress would overrun the allocation of reduced ascorbate, the rate of threonate would increase, due to a failure in the ascorbate recycling process (Baxter *et al*. 2007, Shulaev *et al*. 2008). However, on DOE 16 the content of ascorbate was not significantly higher in the girdle treatment in comparison to control anymore. This may indicate that oxidative stress was transient and with a further development of the leaves, overexcitation was no longer a problem. The late accumulation of glucose and fructose, despite the early decrease of photosynthesis, could be due to a late tailback, because of an initial transport (*via* sucrose) of the photosynthetic metabolites into the twig. Sugars and other osmolytes are not only known to regulate osmotic potential, but also to operate as 'osmoprotectants' for enzymes and membranes (Le Rudulier *et al*. 1984, Shen *et al*. 1997, Sardans *et al*. 2014).

In *Arabidopsis* the contents of the hexoses, glucose and fructose, rise drastically, while the sucrose content is more stable in senescing leaves (Quirino *et al*. 2001). Although a decrease in photosynthetic rates and an increase of the soluble carbohydrates fructose and glucose could be detected, no signs for senescence induction in the leaves of downy oak were found in the present study. Neither Chl degradation, nor a dissection of parts of the photosynthetic apparatus could be observed. Clearly visible was a slow-down of the leaf development, with consequences for nearly all parameters of the OJIP-transient and a decline of the antioxidants, ascorbate and citrate. Consequently, sugar accumulation on its own was not one of the main triggers of senescence in downy oak.

References

Barrs H.D., Weatherley P.E.: A re-examination of relative turgidity technique for estimating water deficits in leaves. – Aust. J. Biol. Sci. **15**: 413-428, 1962.

Baxter C.J., Redestig H., Schauer N. *et al*.: The metabolic response of heterotrophic *Arabidopsis* cells to oxidative stress. – Plant Physiol. **143**: 312-325, 2007.

Ceppi M.G., Oukarroum A., Çiçek N. *et al*.: The IP amplitude of the fluorescence rise OJIP is sensitive to changes in the photosystem I content of leaves: a study on plants exposed to magnesium and sulfate deficiencies, drought stress and salt stress. – Physiol. Plantarum **144**: 277-288, 2012.

Doerfler H., Lyon D., Nägele T. *et al*.: Granger causality in integrated GC–MS and LC–MS metabolomics data reveals the interface of primary and secondary metabolism. – Metabolomics **9**: 564-574, 2013.

Gibson S.I.: Control of plant development and gene expression by sugar signaling. – Curr. Opin. Plant Biol. **8**: 93-102. 2005.

Hensel L.L., Grbić V., Baumgarten D.A., Bleecker A.B.: Developmental and age-related processes that influence the longevity and senescence of photosynthetic tissue in *Arabidopsis*. – Plant Cell **5**: 553-564, 1993.

Holland V., Koller S., Brüggemann W.: Insight into the photosynthetic apparatus in evergreen and deciduous European oaks during autumn senescence using OJIP fluorescence transient analysis. – Plant Biol. **16**: 801-808, 2014.

Holland V., Koller S., Lukas S., Brüggemann W.: Drought-and frost-induced accumulation of soluble carbohydrates during accelerated senescence in *Quercus pubescens*. – Trees 215-227, 2015.

Iglesias D.J., Lliso I., Tadeo F.R., Talon M.: Regulation of photosynthesis through source: sink imbalance in citrus is mediated by carbohydrate content in leaves. – Physiol. Plantarum **116**: 563-572, 2002.

Jang J.C., Sheen J.: Sugar sensing in higher plants. – The Plant Cell **6**: 1665-1679, 1994.

Jiang C.D., Jiang G.M., Wang X. *et al*.: Increased photosynthetic activities and thermostability of photosystem II with leaf development of elm seedlings (*Ulmus pumila*) probed by the fast fluorescence rise OJIP. – Environ. Exp. Bot. **58**: 261-268, 2006.

Joly D., Bigras C., Harnois J. *et al*.: Kinetic analyses of the OJIP chlorophyll fluorescence rise in thylakoid membranes. – Photosynth. Res. **84**: 107-112, 2005.

Jongebloed U., Szederkényi J., Hartig K. *et al*.: Sequence of morphological and physiological events during natural ageing and senescence of castor bean leaf: sieve tube occlusion and carbohydrate back-up precede chlorophyll degradation. – Physiol. Plantarum **120**: 338-346, 2004.

Kopka J., Schauer N., Krueger S. *et al*.: GMD@ CSB. DB: the Golm metabolome database. – Bioinformatics **21**: 1635-1638, 2005.

Krapp A., Hofmann B., Schäfer C., Stitt M.: Regulation of the expression of *rbcS* and other photosynthetic genes by carbohydrates: a mechanism for the 'sink regulation' of photosynthesis? – Plant J. **3**: 817-828, 1993.

Krapp A., Stitt M.: An evaluation of direct and indirect mechanisms for the 'sink regulation' of photosynthesis in spinach: changes in gas exchange, carbohydrates, metabolites, enzyme activities and steady-state transcript events after cold-girdling source leaves. – Planta **195**: 313-323, 1995.

Le Rudulier D., Strom A.R., Dandekar A.M. *et al*.: Molecular biology of osmoregulation. – Science **224**: 1064-1068, 1984.

Lichtenthaler H.K.: Chlorophylls and carotenoids: pigments of photosynthetic biomembranes. – Methods Enzymol. **184**: 350-382, 1987.

Lloyd J.C., Zakhleniuk O.V.: Responses of primary and secondary metabolism to sugar accumulation revealed by microarray expression analysis of the *Arabidopsis* mutant, pho3. – J. Exp. Bot. **55**: 1221-1230, 2004.

Morecroft M.D., Stokes V.J., Morison J.I.L.: Seasonal changes in the photosynthetic capacity of canopy oak (Quercus robur) leaves: the impact of slow development on annual carbon uptake. – Int. J. Biometeorol. **47**: 221-226, 2003.

Noodén L.D., Guiamét J.J.: Regulation of assimilation and senescence by the fruit in monocarpic plants. – Physiol. Plantarum **77**: 267-274, 1989.

Parrott D., Yang L., Shama L., Fischer A.M.: Senescence is accelerated, and several proteases are induced by carbon 'feast' conditions in barley (*Hordeum vulgare* L.) leaves. – Planta **222**: 989-1000, 2005.

Parrott D.L., McInnerney K., Feller U., Fischer A.M.: Steam-girdling of barley (*Hordeum vulgare*) leaves leads to carbohydrate accumulation and accelerated leaf senescence, facilitating transcriptomic analysis of senescence-associated

genes. – New Phytol. **176**: 56-69, 2007.
Patakas A., Noitsakis B.: Leaf age effects on solute accumulation in water-stressed grapevines. – J. Plant Physiol. **158**: 63-69, 2001.
Pinheiro C., Passarinho J.A., Ricardo C.P.: Effect of drought and rewatering on the metabolism of *Lupinus albus* organs. – J. Plant Physiol. **161**: 1203-1210, 2004.
Quirino B.F., Reiter W.D., Amasino R.M.: One of two tandem *Arabidopsis* genes homologous to monosaccharide transporters is senescence-associated. – Plant Mol. Biol. **46**: 447-457, 2001.
Rizhsky L., Liang H.J., Shuman J. *et al.*: When defense pathways collide. The response of *Arabidopsis* to a combination of drought and heat stress. – Plant Physiol. **134**: 1683-1696, 2004.
Sardans J., Peñuelas J., Rivas-Ubach A.: Ecological metabolomics: overview of current developments and future challenges. – Chemoecology **21**: 191-225, 2011.
Sardans J., Gargallo-Garriga A., Pérez-Trujillo M. *et al.*: Metabolic responses of *Quercus ilex* seedlings to wounding analysed with nuclear magnetic resonance profiling. – Plant Biol. **16**: 395-403, 2014.
Sawada S., Arakawa O., Muraki I. *et al.*: Photosynthesis with single-rooted *Amaranthus* leaves. I. Changes in the activities of RuBP-1, 5-bisphosphate carboxylase and phospho*enol*-pyruvate carboxylase and the amounts of intermediates in photosynthetic metabolism in response to changes in the source-sink balance. – Plant Cell Physiol. **40**: 1143-1151, 1999.
Sawada S., Sakamoto T., Sato M. *et al.*: Photosynthesis with single-rooted *Amaranthus* leaves. II. Regulation of ribuelose-1, 5-bisphosphate carboxylase, phospho*enol*pyruvate carboxylase, NAD-malic enzyme and NAD-malate dehydrogenase and coordination between PCR and C4 photosynthetic metabolism in response to changes in the source-sink balance. – Plant Cell Physiol. **43**: 1293-1301, 2002.
Schauer N., Fernie A.R.: Plant metabolomics: towards biological function and mechanism. – Trends Plant Sci. **11**: 508-516, 2006.
Shen B., Jensen R.G., Bohnert H.J.: Increased resistance to oxidative stress in transgenic plants by targeting mannitol biosynthesis to chloroplasts. – Plant Physiol. **113**: 1177-1183, 1997.
Shulaev V., Cortes D., Miller G., Mittler R.: Metabolomics for plant stress response. – Physiol. Plantarum **132**: 199-208, 2008.
Strasser R.J., Srivastava A., Tsimilli-Michael M.: The fluorescence transient as a tool to characterize and screen photosynthetic samples. – In: Yunus M., Pathre U., Mohanty P. (ed.): Probing Photosynthesis: Mechanisms, Regulation and Adaptation. Pp 445-483. Taylor and Francis, London 2000.
Strasser R.J., Tsimilli-Michael M., Srivastava A.: Analysis of the chlorphyll *a* fluorescence transient. – In: Papageorgiou C., Govindjee (ed.): Chlorophyll *a* Fluorescence: A Signature of Photosynthesis. Pp. 321-362. Kluwer Academic, Dordrecht 2004.
Strehmel N., Hummel J., Erban A. *et al.*: Retention index thresholds for compound matching in GC-MS metabolite profiling. – J. Chromatogr. B **871**: 182-190, 2008.
Strivastava A., Strasser R.J.: Greening of peas: parallel measurements of 77 K emission spectra, OJIP chlorophyll a fluorescence transient, period four oscillation of the initial fluorescence level, delayed light emission, and P700. – Photosynthetica **37**: 365-392, 1999.
Webber A.N., Nie G.Y., Long S.P.: Acclimation of photosynthetic proteins to rising atmospheric CO_2. – Photosynth. Res. **39**: 413-425, 1994.
Weckwerth W., Wenzel K., Fiehn O.: Process for the integrated extraction, identification and quantification of metabolites, proteins and RNA to reveal their co-regulation in biochemical networks. – Proteomics **4**: 78-83, 2004.
Wingler A., Roitsch T.: Metabolic regulation of leaf senescence: Interactions of sugar signalling with biotic and abiotic stress responses. – Plant Biol. **10**: 50-62, 2008.
Xiao W., Sheen J., Jang J.C.: The role of hexokinase in plant sugar signal transduction and growth and development. – Plant Mol. Biol. **44**: 451-461, 2000.
Yordanov I.: Structure and functional characteristic of photosynthetic apparatus of bean plants of different biological states, treated with high temperatures and antibiotics. – DrSci Dissertation, Pp. 433, BAS, Sofia 1984.
Yordanov I., Goltsev V., Stefanov D. *et al.*: Preservation of photosynthetic electron transport from senescence-induced inactivation in primary leaves after decapitation and defoliation of bean plants. – J. Plant Physiol. **165**: 1954-1963, 2008.